Chinese Chemical Letters 35 (2024) 108894

Contents lists available at ScienceDirect

Chinese Chemical Letters

journal homepage: www.elsevier.com/locate/cclet

Freezing-directed construction of enzyme/nano interfaces: Reagentless conjugation, superior activity, and better stability

Ke Quan[a,1], Jiajie Tong[a,1], Lifang Chen[a,1], Shuyao Fang[a], Mengjiao Li[a], Linlin Wu[b], Zhihe Qing[a,*]

[a] Hunan Provincial Key Laboratory of Cytochemistry, School of Food and Bioengineering, School of Chemistry and Chemical Engineering, Changsha University of Science and Technology, Changsha 410114, China
[b] Department of Oncology, Tengzhou Central People's Hospital Affiliated Xuzhou Medical University, Tengzhou 277500, China

ARTICLE INFO

Article history:
Received 29 March 2023
Revised 17 July 2023
Accepted 4 August 2023
Available online 5 August 2023

Keywords:
Enzyme conjugation
Freezing
AuNPs
Catalytic activity

ABSTRACT

Immobilizing enzyme to nano interfaces has demonstrated to be a favorable strategy for prompting the industrialized application of enzyme. Despite tremendous endeavor has been devoted to using gold nanoparticles (AuNPs) as conjugation matrix due to its fascinating physico-chemical properties, maintaining enzymatic activity while circumventing cumbersome modification remains a formidable challenge. Herein, the freezing-directed conjugation of enzyme/nano interfaces was constructed without extra reagent. As the proof of concept, glucose oxidase (GOx) was chosen as model enzyme. The one-pot conjugation process can be facilely completed at −20 °C under aqueous solution. Moreover, with the loading of GOx on AuNP at freezing, the enzyme exhibited superior catalytic activity and stability upon thermal and pH perturbation. The mechanism of boosted activity was then discussed in detail. It was found that higher loading density under freezing condition and more enzyme tending to bind AuNPs *via* Au-S bond were the main factors for the superior activity. More importantly, this methodology was universal and can also be applied to other enzyme which contains natural cysteine, such as horseradish peroxidase (HRP) and papain. This facile conjugation strategy accompanied by remarkable bioactivity expand the possibilities for enzymatic biosensing, microdevice and even drug delivery.

Enzymes are extremely crucial as environmentally-friendly and natural catalyst due to their catalyzing features with fascinating efficiency and selectivity. They are widely applied in green chemistry and food industry, in biosensing field as signal amplifiers, even in biomedicine field as therapeutic tools [1,2]. However, the intrinsic fragility of enzymes upon aggressive environments (acid, alkaline, and heat fluctuation), poor recovery greatly restricts their industrialization [3]. Immobilizing enzyme on inert nanomaterials has demonstrated to be a favorable alternative with boosted stability [4] enhanced activity [5] and regeneration [6–8]. Among this, gold nanoparticles (AuNPs) have been identified as ideal matrix for enzyme/nano interfaces bioconjugation with large surface area and comparable size to enzyme [9]. As biocompatible nanomaterials, AuNPs exhibit excellent electronic properties and provide mild environment for enzyme without compromising freedom in orientation [10].

The common technique for generating enzyme/AuNP conjugate was nonspecific adsorption. But the weak interaction and uncontrolled enzyme orientation can result in a loss of enzymatic activity [11]. An alternative strategy exploited amino group of native lysine on protein bounding to carboxylic acid-functionalized AuNPs [12]. Despite AuNP and protein can interact *via* classical Au-S bond, but either the protein required complicated cysteine-tagged modification [13,14] or AuNP needed multi-step functionalization [9]. Though tremendous efforts have been made to develop enzyme/AuNP conjugated methods, there is still in urgent demand for facile approach that preserve enzyme activity while avoiding cumbersome modification.

Recently, Liu *et al.* have realized the reagent-free and efficient labeling of thiolated DNA on AuNP through the "freezing temperatures" approach, which occurred with increased local concentration in a compressed reaction volume [15]. Additionally, our group also expanded the excellence of freezing-based method to bioapplication *via* attaching thiolated DNA to AuNP@Pt [16] and Pt [17] nanoparticles. We then suppose that enzyme's cysteine could be directly interacted to AuNP through Au-S bond under freezing

* Corresponding author.
E-mail address: qingzhihe@hnu.edu.cn (Z. Qing).
[1] These authors contributed equally to this work.

https://doi.org/10.1016/j.cclet.2023.108894
1001-8417/

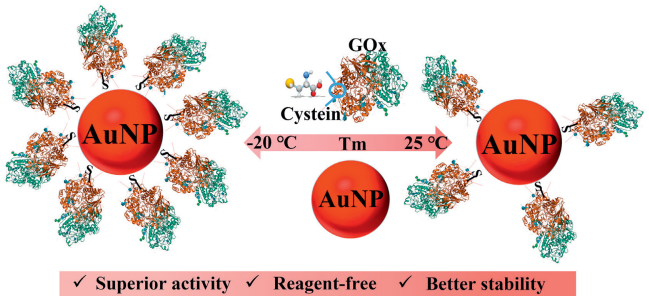

Scheme 1. Illustration of conjugation enzyme to AuNP *via* freezing method. GOx was chosen as the model enzyme and the yellow sphere denoted sulfydryl of natural cystein in GOx.

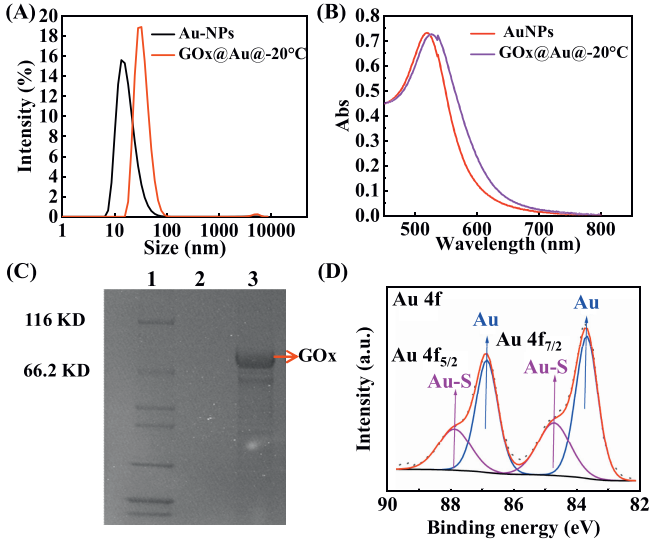

Fig. 1. (A) Size distribution of the AuNPs and GOx@Au@−20 °C. GOx@Au@−20 °C was prepared by conjugating GOx to AuNP at −20 °C for 2 h. (B) UV–vis absorption spectra of the AuNPs, GOx@Au@−20 °C. (C) SDS-PAGE image of GOx@Au@−20 °C conjugate. Lane 1: marker, Lane 2: AuNPs, Lane 3: GOx@Au@−20 °C. (D) XPS spectra line of GOx@AuNP conjugate at freeze temperature (GOx@Au@−20 °C).

temperature without the need for cysteine-tagged modification, thus conjugating enzyme to AuNP can be achieved through one-pot and reagentless strategy. To demonstrate the proof of concept, glucose oxidase (GOx) was chosen as a model enzyme. As shown in Scheme 1, AuNP can serve as supporting matrix to immobilize and stabilize enzyme *via* simply mixing GOx and AuNP under freezing temperature in aqueous solution. With the conjugation of GOx on AuNP at −20 °C, the enzyme possesses superior catalytic activity and stability even under harsh conditions. The one-pot conjugation method accompanied by promoted bioactivity opens up a new avenue to enzyme/nano interface system in challenging real-world application.

To validate the freezing-directed conjugation strategy of enzyme/nano interfaces, GOx was chosen as model enzyme owing to its high turnover and broad application in glucose detection [18], food preservation and even biofuel cells [19]. The AuNPs were synthesized by the standard citrate-reduction method [20] and firstly confirmed by dynamic light scattering (DLS, Fig. 1A) and visible absorption peak at 520 nm (Fig. 1B). After loading GOx on AuNP at −20 °C (GOx@Au@−20 °C), the maximum visible absorption peak shifted from 520 nm to 525 nm, indicating the successful conjugation of protein to nanoparticles [21]. The DLS data presented results which was accordant with absorption spectrum, with hydrodynamic diameter increased from 17±3.2 nm to 35±4.3 nm. Gel

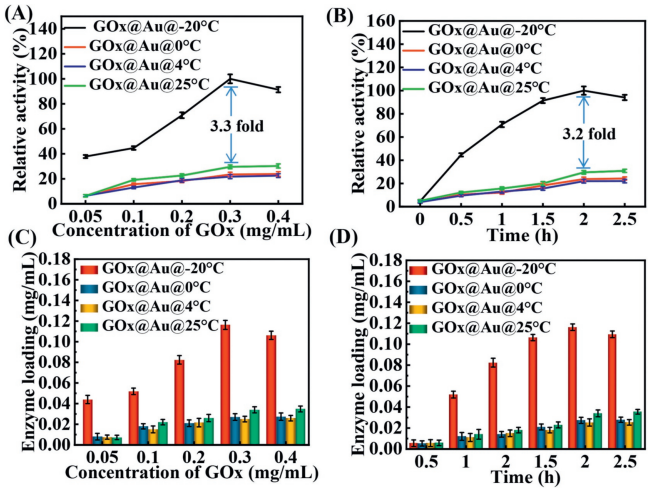

Fig. 2. (A) Relative enzyme activity of GOx@Au@−20 °C, GOx@Au@0 °C, GOx@Au@4 °C and GOx@Au@25 °C after adding different concentrations of free GOx (0.05−0.6 mg/mL). The concentration of AuNPs was fixed at 3 nmol/L. Relative enzymatic activity were recorded as relative percentage of maximum activity which was set as 100%. (B) Relative enzyme activity of various GOx@AuNP conjugates at different times. The concentration of AuNPs and GOx was fixed as 3 nmol/L and 0.3 mg/mL. (C) The loading density of various GOx@AuNP conjugates after adding different concentration of free GOx. (D) The loading density of various GOx@AuNP conjugates at 0–3 h. The error bar represented three parallel experiments.

electrophoresis analysis conducted by SDS-PAGE showed the obvious band at approximately 79 kDa for GOx@Au@−20 °C conjugate (Lane 3, Fig. 1C), corresponding to GOx size and further proved the successful binding GOx on AuNPs.

The well-dispersed and spherical AuNPs in aqueous solution shown in TEM (Fig. S1 in Supporting information) guaranteed a high surface-to-volume ratio for the enzyme conjugation. The introduction of high salt concentration (PBS buffer containing 125 mmol/L NaCl) caused the naked AuNPs to aggregate and solution to appear color change from red to blue. However, no agglomeration of AuNPs was observed at GOx@Au@−20 °C in PBS buffer, suggesting that the GOx in the conjugate might be covalent binding to the AuNP rather than easier-removal adsorption [22]. Then we ulteriorly attempted to clarify the binding force of GOx and AuNP based on the GOx structure. GOx has three cystein (Cys206, Cys521, and Cys164) with one located closely to protein surface: Cys521 [23], which might potentially interact with AuNPs *via* covalent Au-S bond [22]. To verify this hypothesis, furthermore the X-ray photoelectron spectroscopy (XPS) experiment was carried out. The demonstration of binding energy peaks of Au-S $4f_{5/2}$ and Au-S $4f_{7/2}$ at 84.5 and 88.2 eV explicitly evidenced the formation of Au-S bond (Fig. 1D). These results confirmed that this one-pot immobilization strategy was successfully established with GOx as model enzyme and the interaction of GOx and AuNP was mainly through Au-S bond.

The interaction between protein with nanoparticle could cause protein's conformational change as demonstrated by previous studies, which turn out to be influential on protein activity [24]. We further explored whether the function of immobilized enzyme be impacted. The catalytic products of GOx: H_2O_2, with glucose as its substrate, can successively convert 3,3′-dimethoxybenzidine into chromogenic products in the presence of HRP. The enzymatic activity of GOx@AuNP that conjugated at −20 °C (GOx@Au@−20 °C), 0 °C (GOx@Au@0 °C), 4 °C (GOx@Au@4 °C), and 25 °C (GOx@Au@25 °C) thus can be optically measured by visible absorption. Enzyme activity was recorded as relative percentage of maximum activity (set as 100%) in order to minimize possible errors. As shown in Fig. 2A, immobi-

lized enzyme activity under freezing condition dramatically increased to 100% activity in the presence of 0.3 mg/mL free GOx and gradually declined in the presence of 0.4 mg/mL. Kinetic data in Fig. 2B exhibited that GOx@Au@−20 °C fleetly increased to 40% activity after 0.5 h, to 65% after 1 h but enzymatic activities of GOx@Au@0 °C, GOx@Au@4 °C, GOx@Au@25 °C entirely showed less than 10% (0.5 h) and 15% (1 h) activities. Under optimal time (2 h), enzymatic activity of conjugate at −20 °C (100%) were much better preserved than other temperature: 25% (0 °C), 20% (4 °C), and 20% (25 °C). These results indicated that the facile conjugation strategy upon freezing temperature has been established on-demand and possessed fascinating activity.

Then we tried to elucidate the mechanism of superior activity upon freezing temperature. According to previous research, the loading density of enzyme on nano-interface is responsible for its conformational change and steric hindrance, which in turn adjust the access of substrate to catalytic center [25]. Therefore, we speculated that the excellent GOx activity might be related to loading density. Then much efforts have been devoted to determine the protein concentration on AuNPs by the Bradford method [26]. As the concentration of GOx elevated from 1.875×10^{-2} mg/mL to 10 times larger, the absorbance at 595 nm gradually increased with coomassie blue stain (Fig. S2 in Supporting information). Thereafter a satisfied linear fit of the calibration curve was acquired to quantify the GOx. When fixing the concentration of AuNPs to 3 nmol/L, the loading amount of GOx on AuNPs at various temperature was investigated upon increasing free GOx from 0.05 mg/mL to 0.4 mg/mL (Fig. 2C). The loading density of GOx on AuNPs was obviously increased and reached saturation when adding 0.3 mg/mL free GOx. The loading amount of GOx@Au@0 °C, GOx@Au@4 °C, and GOx@Au@25 °C displayed similar results, each only 30% amount of that of the freezing conjugates, evidencing the superior performance of freezing method. Besides the amount of free GOx, the incubation time likewise play decisive role in the loading density. The density in GOx@Au@−20 °C conjugate was dramatically elevated upon extending reaction time and reached plateau at 2 h, whereas conjugation at 0 °C, 4 °C, and 25 °C exhibited much lower loading density in the same condition (Fig. 2D). It may be reasoned according to the previous study that AuNPs, GOx will be pushed out of the gradually formed ice crystals upon freezing condition and thus be concentrated in ultra-small space, which prominently boost enzymatic conjugation density [15]. While higher loading density tend to endow greater numbers of catalytic sites each nanoparticle [27], which is directly favourable for enzymatic activity. Therefore, the superior activity might be partly attributed to high loading density under freezing condition. It is worth mentioning that when conjugation density reached to certain levels, the detrimental effect of protein crowding on the substrate approaching to active center may evolve into a new issue [28].

Previous studies have demonstrated that conjugating enzyme to nano interface with specific orientation make advantageous contributions to its activity [11] while the enzymatic activity is compromised by random orientation when interacted to nanoparticles *via* adsorption [29]. On the basis of the specific orientation when GOx binding to AuNPs *via* Au-S bond and the excellent activity under freezing condition, we speculated that the GOx in GOx@Au@−20 °C conjugate was more inclined to interact with AuNPs *via* Au-S bond. To validate this presume, the XPS characteristic of GOx@Au@0 °C, GOx@Au@4 °C, and GOx@Au@25 °C was also conducted (Figs. S3–S5 in Supporting information) and found that the content of Au-S bond at −20 °C was higher than that at other temperatures (Table S1 in Supporting information). Based on the above analysis, we concluded that higher loading density under freezing condition and more enzyme tending to bind AuNPs *via* Au-S bond were the main reasons for the superior enzyme activity.

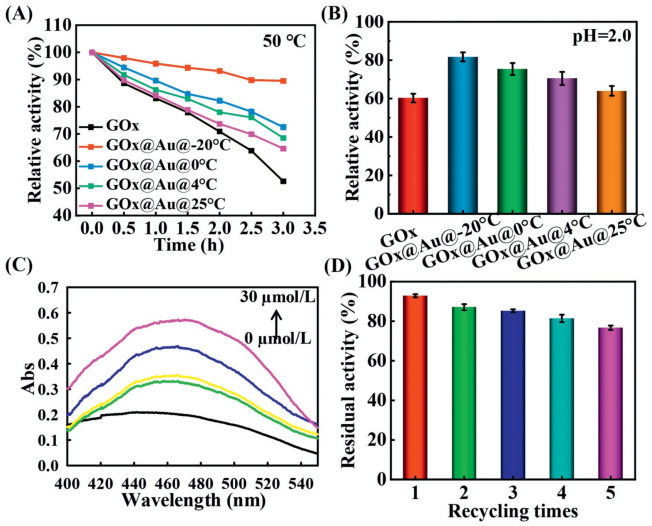

Fig. 3. (A) The relative enzymatic activity of GOx, various GOx@AuNP conjugates after incubated at 50 °C for 0–3 h. The initial activity was recorded as 100% activity. (B) Relative enzyme activity of GOx, various GOx@AuNP conjugates after incubated in phosphate buffer (pH 2.0) for 1 h. (C) The absorption spectra of chromogenic products in the presence of HRP after adding various concentration of glucose to GOx@Au@−20 °C. (D) The residual acitivity of GOx@Au@−20 °C after catalysis of glucose at different recycling times (1–5 times).

After applying GOx@AuNP conjugates in catalysis, the protection effect of AuNPs to enzyme was also investigated under inhospitable environments such as heat, acid and alkaline. First, we evaluated its thermal tolerance by immersing GOx@AuNP conjugates in 50 °C water. After heat treatment for 1 h, free GOx maintain only 83% of original activity while GOx@Au@−20 °C (98%), GOx@Au@4 °C (88%), and GOx@Au@0 °C (90%) retain better activity. When subjected to 50 °C for 3 h, free GOx dramatically decreased to 52% activity, whereas GOx@Au@−20 °C preserved much better activity (91%) and GOx@Au@4 °C, GOx@Au@0 °C, and GOx@Au@25 °C retained moderate activity (70%, 75% and 68%, Fig. 3A). Next, the acid tolerance was investigated in phosphate buffer (pH 2.0). Protective experiment indicated that GOx@Au@−20 °C maintained 80% activity after exposure to acid environment for 1 h but GOx@Au@4 °C, GOx@Au@0 °C, GOx@Au@25 °C showed slightly lower activity and free GOx exhibited only 60% activity (Fig. 3B). A similar effect was generated after alkaline treatment in pH 9.0 for 1 h as evidenced in Fig. S6 (Supporting information). These results suggested that AuNPs afforded as a splendid “shielding” material for GOx upon external perturbation. To evaluate its practical application potential, stability of GOx@Au@−20 °C conjugate at different pH (pH 4.0–9.0) and storage times (0–30 days) was subsequently investigated. Negligible size change characterized by DLS (Fig. S7 in Supporting information) and TEM (Fig. S8 in Supporting information) was observed when storage time prolonged even for 30 days. Even if the storage days extended to 60 days, the enzyme activity still remained above 80% activity (Fig. S9 in Supporting information). Similar results were obtained when incubated GOx@Au@−20 °C at different pH for 1 h, which exhibited distinguished stability (Figs. S10 and S11 in Supporting information). Finally, we examined the catalytic reusability of GOx@AuNP conjugate, which is a vital indicator for industrial biocatalysts [30]. The sensing performance of the GOx@Au@−20 °C conjugate was firstly proved by the increased absorption when the concentration of glucose varied from 5 μmol/L to 30 μmol/L (Fig. 3C). Then it could be easily reused through centrifugation and recycled five times without significant activity reduction (Fig. 3D). Finally, the practicability of immobilized GOx for

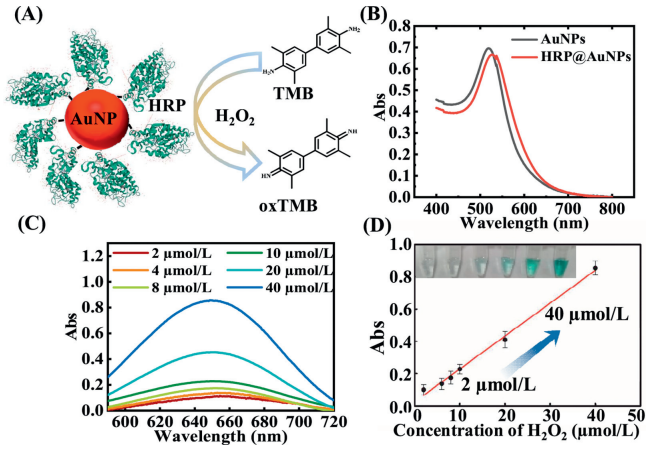

Fig. 4. (A) Schematic description of conjugating AuNPs to horseradish peroxidase (HRP) and its catalytic reaction with TMB. (B) UV–vis absorption spectra of the AuNP and HRP@AuNP. The HRP@AuNP was prepared by incubating HRP with AuNP at −20 °C for 2 h. (C) The absorption spectra of oxTMB in the presence of HRP after adding various concentration of H_2O_2 (2–40 μmol/L) to GOx@Au@−20 °C. (D) Linear regression equation between absorbance at 652 nm and H_2O_2 concentration. The insert pictures showed the corresponding photograph.

glucose detection in glucose-free tea was investigated (Table S2 in Supporting information), which exhibited satisfactory recovery.

Encouraged by the features of facile conjugation, superior catalytic activity and boosted stability of the aforementioned freezing strategy, we further sought to evaluate its generality, with papain as chosen representative. Papain is one model of cysteine-proteases and widely used in industrial field such as food industries, drug production [31]. After free papain incubated with AuNP under freezing conditions for 2 h, the absorbance measured by Bradford assay first increased and then decreased accompanying the free papain amount vary from 0 to 0.4 mg/mL, which was consistent with GOx and confirmed the successful loading papain on AuNP (Fig. S12 in Supporting information). Furthermore, the observation of binding energy peaks of Au-S $4f_{5/2}$ and Au-S $4f_{7/2}$ at 84.5 eV and 88.2 eV using XPS verified the formation of Au-S bond (Fig. S13 in Supporting information). Then HRP, a commonly used enzyme, was also selected as model protein and the sensing mechanism was shown in Fig. 4A. The red shift of maximum absorption wavelength suggested the accomplished loading of HRP on AuNP (Fig. 4B). We thereafter investigated its catalytic property that catalyzed oxidation of 3,3′,5,5′-tetramethylbenzidine (TMB) to oxTMB for colorimetric analysis in the presence of H_2O_2. As the concentration of H_2O_2 elevated from 2 μmol/L to 40 μmol/L, the absorbance at 652 nm gradually increased (Fig. 4C) and the color of solution changed from colorless to blue (Fig. 4D). The concentration of H_2O_2 has a good linear relationship with the absorbance at 652 nm as displayed in Fig. 4D, indicating that the conjugated HRP has satisfactory potential in biosensing. Similarly, tap water and lake water were selected for spiked recovery tests to assess the detection capability of HRP@AuNP in real samples (Table S3 in Supporting information). The results of the spiked recovery experiments indicated that the HRP@AuNP was of good accuracy.

In summary, we have developed a freezing-directed approach to construct enzyme/nano interface. This facile and general strategy combines the merits of immobilized enzyme with distinguished physico-chemical properties of AuNP, which exhibits superior activity and high stability. It has remarkable advantages over previous methods in the following aspects: (1) It is a one-pot conjugated strategy and no extra reagent are needed. (2) The resulting enzyme/AuNP conjugate harbours excellent stability against external heat and pH perturbations. (3) Finally, this method is universal and can be extended to other cysteine-containing enzyme such as HRP and papain. We anticipate that such conspicuous advances will be exploited to construct enzyme/nano interface for biosensing, microdevice and drug delivery.

Declaration of competing interest

The authors declare that they have no known competing financial interests or personal relationships that could have appeared to influence the work reported in this paper.

Acknowledgments

This work was supported by the National Natural Science Foundation of China (Nos. 32001782 and 22222402), the Natural Science Foundation of Hunan Province (No. 2021JJ40564), Changsha Municipal Natural Science Foundation (No. kq2007021), the Opening Foundation of State Key Laboratory of Chemo/Biosensing and Chemometrics, Hunan University (No. 2019013), and Open Project of State Key Laboratory of Supramolecular Structure and Materials (No. sklssm2023016).

Supplementary materials

Supplementary material associated with this article can be found, in the online version, at doi:10.1016/j.cclet.2023.108894.

References

[1] R. Chapman, M.H. Stenzel, J. Am. Chem. Soc. 141 (2019) 2754–2769.
[2] Y.S. Mao, C.F. Zou, Y.J. Jiang, et al., Chin. Chem. Lett. 32 (2021) 990–998.
[3] V.M. Balcao, M.M.D.C. Vila, Adv. Drug Deliv. Rev. 93 (2015) 25–41.
[4] G.R. Cheng, J.P. Xing, Z.F. Pi, et al., Chin. Chem. Lett. 30 (2019) 656–659.
[5] X.G. Yang, J.R. Zhang, X.K. Tian, et al., Angew. Chem. Int. Ed. 62 (2023) e202216699.
[6] F. Shi, J.M. Xu, Z.F. Hu, et al., Chin. Chem. Lett. 32 (2021) 3185–3188.
[7] J. Qiao, L.L. Liu, J. Shen, L. Qi, Chin. Chem. Lett. 32 (2021) 3195–3198.
[8] R.A. Sheldon, A. Basso, D. Brady, Chem. Soc. Rev. 50 (2021) 5850–5862.
[9] A.V. Ramsey, A.J. Bischoff, M.B. Francis, J. Am. Chem. Soc. 143 (2021) 7342–7350.
[10] J.J. Feng, G. Zhao, J.J. Xu, et al., Anal. Biochem. 342 (2005) 280–286.
[11] F. Liu, L. Wang, H.W. Wang, et al., ACS Appl. Mater. Interfaces 7 (2015) 3717–3724.
[12] K.A. Mahmoud, K.B. Male, S. Hrapovic, et al., ACS Appl. Mater. Interfaces 7 (2009) 1383–1386.
[13] L.R. Ditzler, A. Sen, M.J. Gannon, et al., J. Am. Chem. Soc. 133 (2011) 13284–13287.
[14] M.E. Aubin-Tama, W. Hwang, K. Hamad-Schifferli, Proc. Natl. Acad. Sci. U. S. A. 106 (2009) 4095–4100.
[15] B.W. Liu, J.W. Liu, J. Am. Chem. Soc. 139 (2017) 9471–9474.
[16] Z.H. Qing, G.Y. Luo, S.H. Xing, et al., Angew. Chem. Int. Ed. 59 (2020) 14044–14048.
[17] L.F. Chen, S.H. Xing, Y.L. Lei, et al., Angew. Chem. Int. Ed. 60 (2021) 23534.
[18] X. Sun, Y. Li, Q. Yang, et al., Chin. Chem. Lett. 32 (2021) 1780–1784.
[19] A.A. Babadi, S. Bagheri, S.B.A. Hamid, Biosens. Bioelectron. 79 (2016) 850–860.
[20] J. Liu, Y. Lu, Nat. Protoc. 1 (2006) 246–252.
[21] E. Casals, T. Pfaller, A. Duschl, et al., ACS Nano 4 (2010) 3623–3632.
[22] J.M. Lee, H.K. Park, Y.W. Jung, et al., Anal. Chem. 79 (2007) 2680–2687.
[23] E. Tellechea, K.J. Wilson, E. Bravo, et al., Langmuir 28 (2012) 5190–5200.
[24] P. Roach, D. Farrar, C.C. Perry, J. Am. Chem. Soc. 128 (2006) 3939–3945.
[25] B.J. Johnson, W.R. Algar, A.P. Malanoski, et al., Nano Today 9 (2014) 102–131.
[26] M.M. Bradford, Anal. Biochem. 72 (1976) 248–254.
[27] Y. Wang, R. Jonkute, H. Lindmark, et al., Langmuir 36 (2020) 37–46.
[28] I.M. Kuznetsova, K.K. Turoverov, V.N. Uversky, Int. J. Mol. Sci. 15 (2014) 23090–23140.
[29] L.S. Wong, F. Khan, J. Micklefield, Chem. Rev. 109 (2009) 4025–4053.
[30] W.B. Liang, H.S. Xu, F. Carraro, et al., J. Am. Chem. Soc. 141 (2019) 2348–2355.
[31] P.V.G. Tacias, S.R. Morellon, V.D. Castaneda, et al., Int. J. Biol. Macromol. 188 (2021) 94–113.